Environmental Science & Technology

Article

pubs.acs.org/est

Observational Insights into Aerosol Formation from Isoprene

David R. Worton,[*,†,‡] Jason D. Surratt,[§] Brian W. LaFranchi,[∥,%] Arthur W. H. Chan,[†] Yunliang Zhao,[†] Robin J. Weber,[†] Jeong-Hoo Park,[†,∫] Jessica B. Gilman,[⊥,#] Joost de Gouw,[⊥,#] Changhyoun Park,[¶,⊗] Gunnar Schade,[¶] Melinda Beaver,[□,⊕] Jason M. St. Clair,[□] John Crounse,[□] Paul Wennberg,[□] Glenn M. Wolfe,[■,°] Sara Harrold,[■] Joel A. Thornton,[■] Delphine K. Farmer,[⊥,○,ϕ] Kenneth S. Docherty,[⊥,○,∂] Michael J. Cubison,[⊥,○,‡] Jose-Luis Jimenez,[⊥,○] Amanda A. Frossard,[●] Lynn M. Russell,[●] Kasper Kristensen,[△] Marianne Glasius,[△] Jingqiu Mao,[▲,▽] Xinrong Ren,[▼] William Brune,[⬡] Eleanor C. Browne,[∥,+] Sally E. Pusede,[∥] Ronald C. Cohen,[∥] John H. Seinfeld,[⬢] and Allen H. Goldstein[†,$]

[†]Department of Environmental Science, Policy and Management, [∥]Department of Chemistry, University of California, Berkeley, California 94720, United States

[‡]Aerosol Dynamics Inc., Berkeley, California 94710, United States

[§]Department of Environmental Sciences and Engineering, Gillings School of Global Public Health, University of North Carolina at Chapel Hill, Chapel Hill, North Carolina 27599, United States

[⊥]Cooperative Institute for Research in the Environmental Sciences, [○]Department of Biochemistry and Chemistry, University of Colorado, Boulder, Colorado 80309, United States

[#]NOAA Earth System Research Laboratory, Boulder, Colorado 80305, United States

[¶]Department of Atmospheric Sciences, Texas A&M University, College Station, Texas 77843, United States

[□]California Institute of Technology, Pasadena, California 91125, United States

[■]Department of Chemistry, University of Washington, Seattle, Washington 98195, United States

[●]Scripps Institution of Oceanography, University of California, San Diego, La Jolla, California 92037, United States

[△]Department of Chemistry, University of Aarhus, Aarhus, DK-8000, Denmark

[▲]Department of Atmospheric and Oceanic Sciences, Princeton University, Princeton, New Jersey 08544, United States

[▽]Geophysical Fluid Dynamics Laboratory, NOAA, Princeton, New Jersey 08540, United States

[▼]Air Resources Laboratory, NOAA, College Park, Maryland 20740, United States

[⬡]Department of Meteorology, Pennsylvania State University, University Park, Pennsylvania 16802, United States

[⬢]Departments of Environmental Science and Engineering and Chemical Engineering, California Institute of Technology, Pasadena, California 91125, United States

[$]Department of Civil and Environmental Engineering, University of California, Berkeley, California 94720, United States

[%]Now at Atmospheric Earth and Energy Division, Lawrence Livermore National Laboratory, Livermore, California 94550, United States

[⊗]Now at Department of Atmospheric Environmental Sciences, Pusan National University, Busan, South Korea

[∫]Now at Institute of Arctic and Alpine Research, University of Colorado, Boulder, Colorado 80309, United States

[⊕]Now at National Exposure Research Laboratory, Environmental Protection Agency, Research Triangle Park, North Carolina 27711, United States

[°]Now at Joint Center for Earth Systems Technology, University of Maryland and NASA Goddard Space Flight Center, Greenbelt, Maryland 20771, United States

[ϕ]Now at Department of Chemistry, Colorado State University, Fort Collins, Colorado 80523, United States

[∂]Now at ToFWerk AG, Thun, CH-3600, Switzerland

[‡]Now at Environmental Alion Science and Technology, EPA Office of Research and Development, EPA Research and Development, Research Triangle Park, North Carolina 27703, United States

[+]Now at Department of Civil and Environmental Engineering, Massachusetts Institute of Technology, Cambridge, Massachusetts 02139, United States

Supporting Information

Received: March 12, 2013
Revised: August 1, 2013
Accepted: September 4, 2013
Published: September 4, 2013

dx.doi.org/10.1021/es4011064 | Environ. Sci. Technol. 2013, 47, 11403−11413

ABSTRACT: Atmospheric photooxidation of isoprene is an important source of secondary organic aerosol (SOA) and there is increasing evidence that anthropogenic oxidant emissions can enhance this SOA formation. In this work, we use ambient observations of organosulfates formed from isoprene epoxydiols (IEPOX) and methacrylic acid epoxide (MAE) and a broad suite of chemical measurements to investigate the relative importance of nitrogen oxide (NO/NO_2) and hydroperoxyl (HO_2) SOA formation pathways from isoprene at a forested site in California. In contrast to IEPOX, the calculated production rate of MAE was observed to be independent of temperature. This is the result of the very fast thermolysis of MPAN at high temperatures that affects the distribution of the MPAN reservoir (MPAN / MPA radical) reducing the fraction that can react with OH to form MAE and subsequently SOA ($F_{MAE\ formation}$). The strong temperature dependence of $F_{MAE\ formation}$ helps to explain our observations of similar concentrations of IEPOX-derived organosulfates (IEPOX-OS; ~1 ng m^{-3}) and MAE-derived organosulfates (MAE-OS; ~1 ng m^{-3}) under cooler conditions (lower isoprene concentrations) and much higher IEPOX-OS (~20 ng m^{-3}) relative to MAE-OS (<0.0005 ng m^{-3}) at higher temperatures (higher isoprene concentrations). A kinetic model of IEPOX and MAE loss showed that MAE forms 10−100 times more ring-opening products than IEPOX and that both are strongly dependent on aerosol water content when aerosol pH is constant. However, the higher fraction of MAE ring opening products does not compensate for the lower MAE production under warmer conditions (higher isoprene concentrations) resulting in lower formation of MAE-derived products relative to IEPOX at the surface. In regions of high NO_x, high isoprene emissions and strong vertical mixing the slower MPAN thermolysis rate aloft could increase the fraction of MPAN that forms MAE resulting in a vertically varying isoprene SOA source.

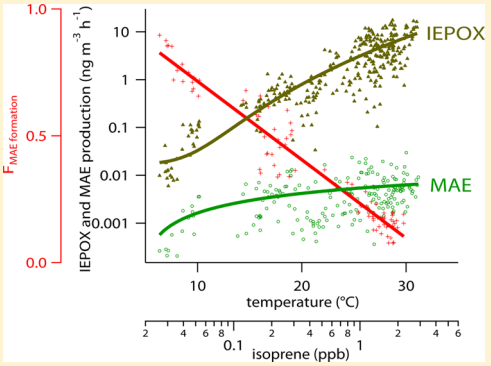

INTRODUCTION

Atmospheric aerosols have adverse effects on human health and air quality and influence Earth's climate.[1] A substantial fraction are secondary organic aerosols (SOA) formed in the atmosphere by oxidation of volatile organic compounds (VOCs).[2] Recent work has shown that SOA formed from biogenic VOCs can be substantially enhanced in polluted air.[3,4] Modeling studies indicate that more than half of biogenic SOA, of which isoprene is a major contributor, could be moderated by controlling anthropogenic emissions.[5,6] Several probable explanations for the anthropogenic enhancement of biogenic SOA have been suggested: (i) enhanced gas to particle partitioning of semivolatile oxidation products onto pre-existing anthropogenic primary and secondary particles,[5] (ii) enhanced uptake of reactive species by acidic aerosols,[7] (iii) oxidation by the nitrate radical (NO_3),[8] and (iv) influence of nitrogen oxide ($NO_x = NO + NO_2$) concentrations on both SOA yields and enhancing oxidant (i.e., hydroxyl radical; OH) concentrations.[5,9]

Isoprene is emitted from vegetation and is the single largest source of VOCs to the atmosphere with global emissions of ~500 Tg C yr^{-1}.[10] In the atmosphere, isoprene reacts predominantly with OH[11] forming SOA with a yield of 1−4% under low NO_x (NO_x < 0.1 ppb),[12] 1−6% under high NO_x (NO_x > 1 ppb),[13,14] and up to 29% in the presence of highly acidic seed aerosols,[15] making it an important source of SOA. In smog chamber experiments, SOA yields were observed to be dependent on NO_x concentrations, the VOC/NO_x ratio, the NO_2/NO ratio and aerosol acidity,[7,9,13,15] consistent with an anthropogenic−biogenic coupling.

Isoprene epoxydiols (IEPOX), oxidation products of the isoprene hydroxyl hydroperoxides (ISOPOOH), and the methacrylic acid epoxide (MAE), an oxidation product of peroxymethylacrylic nitric anhydride (MPAN), have been identified as key gas-phase intermediates to isoprene SOA formation from the hydroperoxyl (HO_2) and nitrogen oxides (NO/NO_2) pathways, respectively.[16,17] The MPAN precursor, MACR, has also been shown to form via the HO_2 channel although the reported yield was an order of magnitude less than the NO/NO_2 channel.[18] Reactive uptake of IEPOX through acid-catalyzed ring-opening reactions has been shown to form known SOA components from the HO_2 pathway, including the 2-methyltetrols, C_5-alkene triols, 3-methyltetrahydrofuran-3,4-diols, IEPOX-derived organosulfates, and oligomers comprising IEPOX monomers.[15,19−21] Further oxidation of MPAN by OH forms MAE, which undergoes acid catalyzed reactive uptake to form known SOA components from the NO/NO_2 pathway, 2-methylglyceric acid (2-MG), MAE-derived organosulfates and oligoesters composed of 2-MG monomers.[15,17,20,22−24]

The role of MPAN has been confirmed by the compositional consistency of SOA formed in laboratory smog chamber photooxidation of isoprene, methacrolein (MACR), and MPAN and as a result of the strong dependence of the isoprene high-NO_x SOA yield on the NO_2/NO ratio that favors MPAN formation.[13,15] Understanding SOA formation from MPAN is important as 2-MG and its derivatives are considered major SOA products of the NO/NO_2 channel and only form through MPAN oxidation. Formation of other products from isoprene oxidation may occur under high NO_x conditions, e.g., glyoxal (yield ~2%) and methyl glyoxal, which can contribute to SOA through aqueous phase processing, though the importance of this chemistry remains uncertain.[25−27]

Figure 1 shows the mechanism, elucidated by recent laboratory work, for formation of the IEPOX-[15,16] and MAE-derived organosulfates[13,15,17] from the HO_2 and NO/NO_2 pathways, respectively. The organosulfates formed from IEPOX and MAE only form through ring-opening epoxide chemistry, due to kinetic limitations of the sulfate alcohol esterification reaction,[28] and have been speculated to be among the products responsible for the enhancement of SOA under acidic conditions.[7,15] Although they are not the only products, they can be utilized as SOA tracers of this acid catalyzed ring-opening chemistry, because with sulfate concentrations of typical atmospheric aerosols, they are major ring-opening products (20−40%)[29] and are expected to be stable in the particle phase due to their low hydrolysis rates and low vapor pressures.[30]

The importance of aerosol acidity for enhancing ambient biogenic SOA formation remains uncertain due to the stronger acidities used in dry laboratory studies relative to those observed in the ambient atmosphere.[31] However, highly acidic seed aerosols are hygroscopic, which does not preclude a role for particle phase

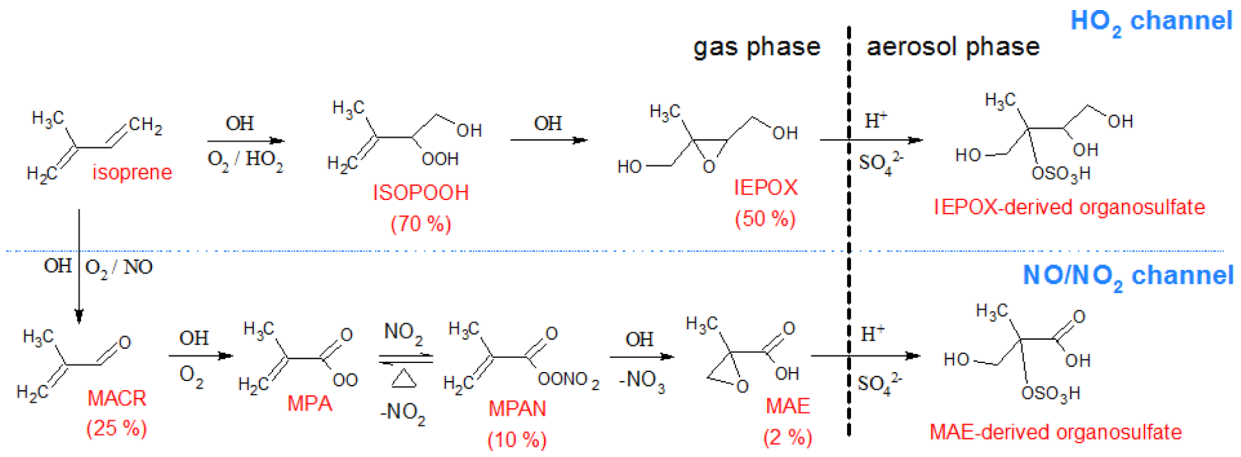

Figure 1. Reaction mechanism, elucidated by recent laboratory work, for the formation of the IEPOX- and MAE-derived organosulfates from isoprene photooxidation for the HO_2 and NO/NO_2 channels, respectively.[13−16] For simplicity, only single isomers and not all reaction pathways are shown. Approximate yields for major products are shown in parentheses.

water in the reactive uptake process. The presence of liquid water in ambient aerosol may mitigate the necessity for very strong aerosol acidities.

It is important to understand the roles of aerosol acidity, aerosol water, and NO_x concentrations on isoprene SOA formation in the ambient atmosphere to further improve their representation in atmospheric models. In this study we use ambient observations of the IEPOX- and MAE-derived organosulfates along with a comprehensive suite of chemical measurements obtained during the Biosphere Effects on Aerosols and Photochemistry Experiment (BEARPEX) to investigate the relative importance of the NO/NO_2 and HO_2 pathways for SOA formation from isoprene under atmospheric conditions.

EXPERIMENTAL SECTION

Filter Collection. Ambient aerosol samples ($PM_{2.5}$, aerosol with aerodynamic diameters of $\leq$2.5 μm) were collected for two continuous 5-day periods in 2007 (20th − 25th September) and 2009 (26th − 31st July) during BEARPEX. The sampling inlet was located at 9.3 m on the main north tower above the canopy of a ponderosa pine (*Pinus ponderosa* L.) plantation owned by Sierra Pacific Industries adjacent to the University of California − Blodgett Forest Research Station (UC-BFRS; 38.90° N, 120.63° W, 1315 m elevation above sea level).[32] The site is located midway between Sacramento, CA, and Carson City, NV, in the Sierra Nevada Mountains and was established as an atmospheric measurement site in 1997.[33] As a result of strong orographic forcing, the daily pattern of winds impacting the Blodgett Forest site are nearly constant in speed and direction all year long.[34] Upslope flow brings anthropogenic pollution from Sacramento and the San Joaquin Valley over a 30 km wide band of isoprene emitting oak trees located on the foothills several hours upwind, making the Blodgett Forest site an ideal location to study the influence of anthropogenic emissions on biogenic SOA formation from isoprene.[35] Further details of the filter collection methodology are given in the Supporting Information.

Filter Analyses. Aliquots (100 cm^2) of all filters were solvent extracted and analyzed by ultraperformance liquid chromatography coupled to electrospray ionization high-resolution time-of-flight mass spectrometry (UPLC/ESI-HR-TOFMS) at the California Institute of Technology.[36] The IEPOX- and MAE-derived organosulfates were detected as deprotonated ions in the negative ion mode using reverse-phase chromatography and were calibrated to the response of an authentic standard of 1,3,4-trihydroxybutan-2-yl hydrogen sulfate (BEPOX-derived organosulfate), which is an appropriate standard for these compounds because differences in ESI response factors for compounds of similar functionality and retention time are expected to be less than a factor of 2−3 based on prior studies (e.g., ref 37). Calibration curves are shown in the Supporting Information (Figure S1). The IEPOX- and MAE-derived organosulfates coelute in the LC system (retention times of 0.95 and 0.96 minutes, respectively) and were separated by extracting the specific deprotonated molecular ions, 215.0225 ± 0.02 and 198.9912 ± 0.02 for the IEPOX- and MAE-derived organosulfates, respectively. The three IEPOX- derived organosulfate isomers were not chromatographically separated from each other and are reported as a sum in this work. Similarly, the two MAE-derived organosulfate isomers were not chromatographically separated and are also reported as a sum.

Other Measurements. A broad suite of environmental parameters, including temperature, relative humidity, photosynthetically active radiation, and ozone, were made during both campaigns.[33] Isoprene and MACR were measured by gas chromatography mass spectrometry (GC/MS) in 2007[38] and gas chromatography flame ionization detection (GC/FID) in 2009.[39,40] The GC/MS and GC/FID calibration scales were shown to be similar following intercomparisons to proton transfer reaction mass spectrometry (PTRMS) measurements made in both years (Figure S2, Supporting Information). Gas-phase IEPOX and ISOPOOH were measured in 2009 using a chemical ionization triple quadrupole mass spectrometer (CIMS).[16] IEPOX and ISOPOOH were also measured in 2007 using a single quadrupole CIMS that could not distinguish between them and they were not calibrated due to a lack of authentic standards at that time. The IEPOX data in 2009 is the sum of both IEPOX isomers because they are detected as a combined signal with the CIMS technique. MPAN was measured using a thermal dissociation CIMS instrument.[41] Gas phase nitric acid (HNO_3) was measured by CIMS in 2007 and laser induced fluorescence (LIF) in 2009.[42,43] NO_2 was measured at several heights during both campaigns using LIF[44,45] and in this work measurements from the 9.3 m height were used. In 2009, NO was also measured using a custom-built chemiluminescence instrument.[46,47] OH was measured by laser induced fluorescence (LIF) at low pressure and HO_2 was converted to OH through its reaction with NO prior to detection by LIF.[48] Total OH reactivity was measured by

observing the decay rate of OH when exposed to ambient air.[49] Further details of the OH measurements are given in the Supporting Information.

Particle number and size distributions were measured during both campaigns using scanning mobility particle sizers (SMPS; TSI model 3936). In 2007, chemically speciated measurements of total organics, sulfate, nitrate, ammonium, and chloride were made using a high resolution aerosol time-of-flight mass spectrometer (AMS-HR-TOFMS, Aerodyne Research Inc.).[50] In 2009, no AMS was deployed, but Teflon filters were collected three times a day for 6 (day) or 12 h (night) and analyzed for total organic aerosol and functional group classes by Fourier transform infrared spectroscopy (FTIR).[51] Aliquots of the high volume filters were analyzed at the University of Aarhus for inorganic ions (ammonium, nitrate, sulfate, and chloride) using a Metrohm ion chromatograph equipped with a Metrosep A Supp 5 column for anions. There was very good agreement between the AMS and the sum of the FTIR and IC measurements following an intercomparison to SMPS measurements (Figure S3, Supporting Information) indicating that they can be directly compared to contrast the aerosol loadings between the two campaigns.

Acyl Peroxy Nitrate (APN) Steady State Model. A steady state model of acyl peroxy radicals[52] constrained by measurements of methacrolein, OH, HO_2, NO, NO_2, and temperature from both BEARPEX campaigns was employed. In 2007, NO was not measured and concentrations were inferred by assuming a photostationary state relationship between NO_2, ozone, and total peroxy radicals (HO_2+RO_2). The RO_2 concentrations were estimated through a separate steady state relationship between HO_2, NO and the total alkyl radical formation determined from the OH reactivity measurements. In 2007, the steady state equations for NO and RO_2 were solved iteratively until values of NO and RO_2 were obtained within convergence criteria of <1%. Further details are given in the Supporting Information. The fraction of MPAN that reacts with OH to form MAE (the NO/NO_2 SOA formation channel) relative to the total loss of the MPA radical to reaction with NO, HO_2, and RO_2 ($F_{MAE\ formation}$) describes the fate of the MPAN reservoir species and is given by

$$F_{\mathrm{MAE\ formation}} = (k_{\mathrm{MPAN+OH}}[\mathrm{MPAN}][\mathrm{OH}]) / (k_{\mathrm{MPAN+OH}}[\mathrm{MPAN}][\mathrm{OH}]) + (k_{\mathrm{MPA+NO}}[\mathrm{MPA}][\mathrm{NO}] + k_{\mathrm{MPA+HO2}}[\mathrm{MPA}][\mathrm{HO_2}] + k_{\mathrm{MPA+RO2}}[\mathrm{MPA}][\mathrm{RO_2}]) \quad (1)$$

Extended Aerosol Inorganics Model (E-AIM). The pH and liquid water content (LWC) of the aerosol phase were calculated using the Extended Aerosol Inorganics Model (E-AIM model II, http://www.aim.env.uea.ac.uk/aim/aim.php)[53,54] constrained by measurements of temperature, relative humidity, particle phase nitrate, sulfate, and ammonium. All solid formation was suppressed in the model and no organic compounds were included. Although predicting aerosol pH can be highly uncertain,[55] Ellis et al. (*manuscript in preparation,* 2013) showed this uncertainty could be substantially reduced by measuring both aerosol ions and gas phase ammonia. Similar to this method, we use gas phase nitric acid in place of gas phase ammonia to constrain the gas to particle partitioning and thus minimize the uncertainty in the calculated aerosol pH. Several studies have suggested that inclusion of organic species in the calculation of aerosol LWC changes predicted values by less than 20%.[56,57] In one study inclusion of organic acids in the E-AIM calculation had very little effect on the predicted LWC (<3%).[58] Inputs of free H^+ concentrations were calculated based on the charge balance from the sulfate, nitrate, and ammonium measurements. Total nitrate in the system was determined by summing the gas phase nitric acid and particle phase nitrate measurements, which the model was then free to partition. A comparison of the modeled and observed gas phase nitric acid demonstrates that the partitioning is well represented by the model (within 10% in 2007 and 50% in 2009) (Figure S4, Supporting Information).

RESULTS AND DISCUSSION

Overview of the BEARPEX Campaigns. Table 1 shows a comparison of the relevant meteorological and core chemical measurements for both the BEARPEX filter collection periods. In 2007, the filter sampling took place during the fall season and was characterized by cooler and wetter conditions and reduced photochemistry (lower ozone and OH reactivity) relative to the summer sampling in 2009. Total daytime HO_x concentrations and the HO_2/OH were higher in 2009 while NO concentrations were ∼40% lower, resulting in a higher HO_2/NO ratio (factor of ∼2) favoring formation of ISOPOOH over MACR in 2009 compared with 2007. Figure 2 shows the observed

Table 1. Comparison of daytime (10:00−16:00) Meteorological and Core Chemical Measurements for the Two 5 Day Filter Collection Periods Only[a]

species	BEARPEX 2007 (*September 20th − 25th*)	BEARPEX 2009 (*July 26th − July 31st*)
	measured	
temperature (°C)	11 (9 − 16)	28 (27 − 29)
relative humidity (%)	63 (40 − 94)	29 (26 − 34)
O_3 (ppb)	41 (38 − 51)	55 (50 − 65)
NO (ppt)	98 (71 − 140)[b,c]	64 (53 − 74)
NO_2 (ppt)	330 (160 − 500)[b,c]	260 (210 − 350)
OH (×10^6 molecules cm^{-3})	2.8 (2.2 − 4.6)	3.0 (1.6 − 4.3)[c]
HO_2 (×10^8 molecules cm^{-3})	1.6 (0.9 − 3.2)	3.8 (1.9 − 8.2)[c]
OH reactivity (s^{-1})	3.2 (3.1 − 3.6)	27 (23 − 31)
isoprene (ppb)[d]	0.05 (0.03 − 0.10)	1.6 (1.4 − 2.0)
ISOPOOH (ppb)	*not quantitative*	0.78 (0.53 − 1.1)
IEPOX (ppb)	*not quantitative*	1.0 (0.77 − 1.4)
MACR (ppb)[d]	0.03 (0.01 − 0.09)	0.33 (0.23 − 0.43)
MPAN (ppt)	31 (13 − 58)	35 (25 − 52)[c]
organic aerosol ($\mu g\ m^{-3}$)[e]	2.1 (1.8 − 2.9)	3.4 (2.2 − 4.7)
sulfate aerosol ($\mu g\ m^{-3}$)[e]	0.32 (0.15 − 0.42)	0.55 (0.42 − 0.74)
	calculated	
aerosol sulfate (M)	2.7 (1.6 − 3.2)	1.3 (0.6 − 1.7)
aerosol pH	4.5 (4.2 − 4.9)	4.4 (4.1 − 4.7)
aerosol LWC ($\mu g\ m^{-3}$)	0.6 (0.1 − 0.9)	0.2 (0.1 − 0.3)

[a]The calculated sulfate molarity, aerosol pH and aerosol liquid water content (LWC) are also shown. Data shown are medians (interquartile range). [b]Estimated from steady state analysis: $[NO] = (J_{NO2[NO2]})/((k_{HO2+NO}[HO_2]+k_{RO2+NO}[RO_2]+k_{NO+O3}[O_3]))$. [c]Data were missing for the specific periods of the filter collections due to instrumental problems and so the given values are for the full campaigns with the 2007 data restricted to the later cooler period from September 13th − October 10th that was more representative of filter sampling conditions.[32] [d]GC/MS (2007) and GC/FID (2009), intercompared via PTRMS (Figure S2, Supporting Information). [e]AMS (2007) and FTIR+IC (2009), intercompared via SMPS (Figure S3, Supporting Information).

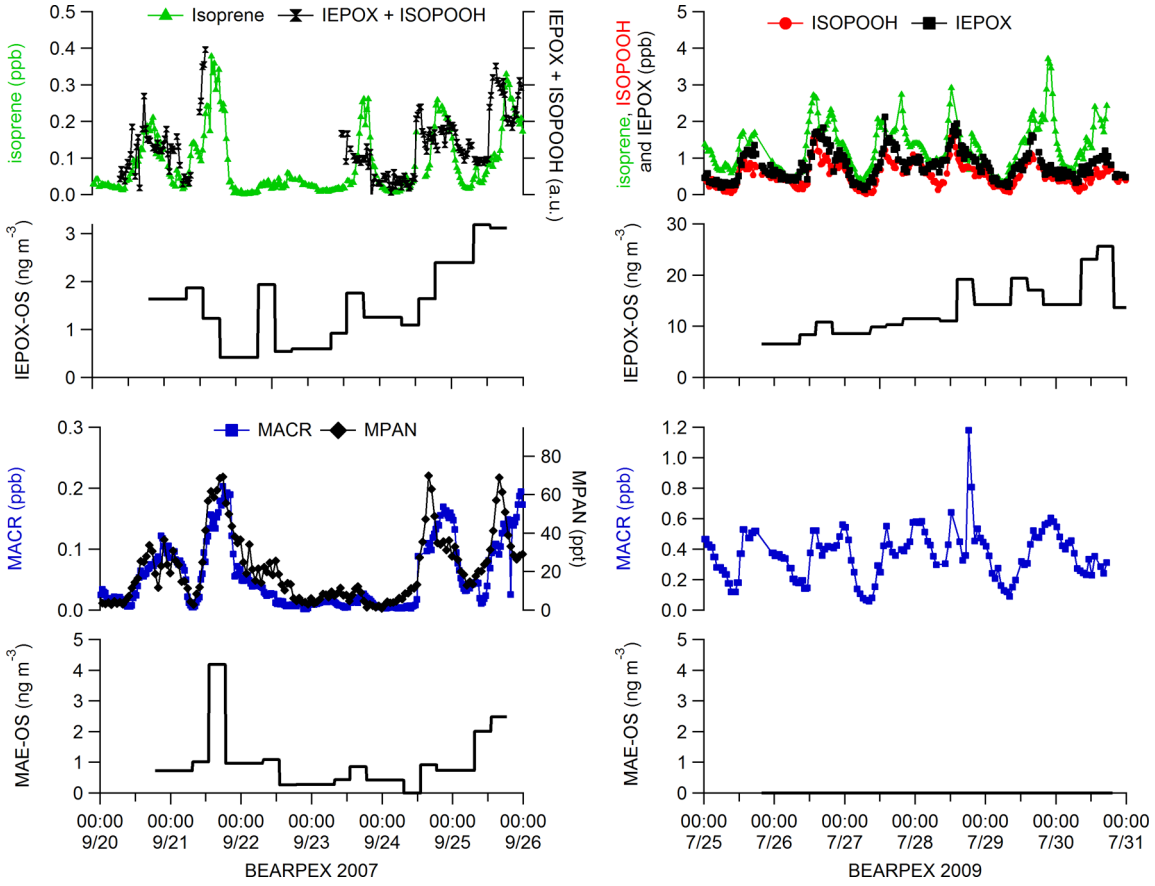

Figure 2. Time series of the IEPOX- and MAE-derived organosulfates (IEPOX OS and MAE OS) and their gas phase precursors, IEPOX and MPAN, for BEARPEX 2007 (left panels) and 2009 (right panels). IEPOX and its precursor ISOPOOH were not calibrated or separated in 2007 and are shown as a sum. ISOPOOH was measured in 2009 and is also shown. There were no coincident MPAN measurements with filter collection in 2009. Isoprene and methacrolein (MACR) are shown for both campaigns. Note the differences in *y*-axis for isoprene (factor of 10), IEPOX-derived organosulfate (factor of 10), and methacrolein (factor of 4) between.

concentrations of isoprene, MACR, ISOPOOH, IEPOX, and the IEPOX- and MAE-derived organosulfates. MAE has only recently been identified[17] and as such no MAE measurements were made during either campaign.

IEPOX and ISOPOOH concentrations in 2009 showed similar diurnal profiles to isoprene and were of a similar magnitude (~1 ppb) with afternoon maxima consistent with the arrival of photochemically processed isoprene from the oak tree source several hours upwind. The diurnal profile of the uncalibrated IEPOX+ISOPOOH signal was less well correlated with isoprene in 2007 as a result of more meteorological variability compared to 2009, which was very consistent day to day (see Figure S5, Supporting Information). Isoprene concentrations were on average a factor of 30 higher during the 2009 filter sampling period relative to 2007 consistent with the higher observed temperatures in 2009 and the known dependences of isoprene emissions.[59] Similar to isoprene, the IEPOX-derived organosulfate concentrations were also higher in 2009 (factor of 10) and contributed ~1% of the total organic and ~3% of the total sulfate aerosol mass, which is substantial for a single group of tracers.

MPAN concentrations in 2007 showed a similar diurnal trend to MACR and were present at average concentrations of ~30 ppt during daytime. There were no coincident MPAN measurements with filter sampling in 2009, but measured concentrations prior to filter collection, when conditions were similar, indicate MPAN was also present at concentrations of ~30 ppt. While MPAN concentrations were similar, the MACR concentrations increased by a factor of 10 between 2007 and 2009. The lower MPAN/MACR ratio in 2009 was the result of the higher thermal dissociation rate at higher temperatures that controls the distribution of the MPAN reservoir by lowering the ratio of MPAN to the MPA radical, as will be shown in the next section. In 2007 concentrations of the MAE-derived organosulfates were of similar magnitude to the IEPOX-derived organosulfates (~1 ng m^{-3}). However, in strong contrast to the large observed increase in the IEPOX-derived organosulfates, the MAE-derived organosulfates were not observed above the detection limit in 2009 (<0.0005 ng m^{-3}; detection limit determined experimentally from injections of known amounts of the BEPOX-derived organosulfate) indicating differences controlling the formation of SOA from the NO/NO_2 and HO_2 pathways.

Role of MPAN Thermal Lifetime for Limiting Isoprene SOA Formation from the NO/NO_2 Pathway. The lifetime of MPAN is dependent on the temperature, the NO/NO_2 ratio and the OH concentration.[52,60] Under warmer temperature conditions (>20 °C) thermal decomposition to the precursor peroxymethacryoyl (PMA) radical and NO_2 is very fast relative to reformation. As a result the loss of MPAN is dominated by reaction of the PMA radical with NO, HO_2, and RO_2, which does not generate known NO/NO_2 channel SOA products. Under cooler conditions (<15 °C), MPAN thermal decomposition is much slower compared to the reformation reaction of the PMA radical with NO_2 and in this situation the reaction with OH can compete with thermal decomposition as a loss pathway for

dx.doi.org/10.1021/es4011064 | Environ. Sci. Technol. 2013, 47, 11403−11413

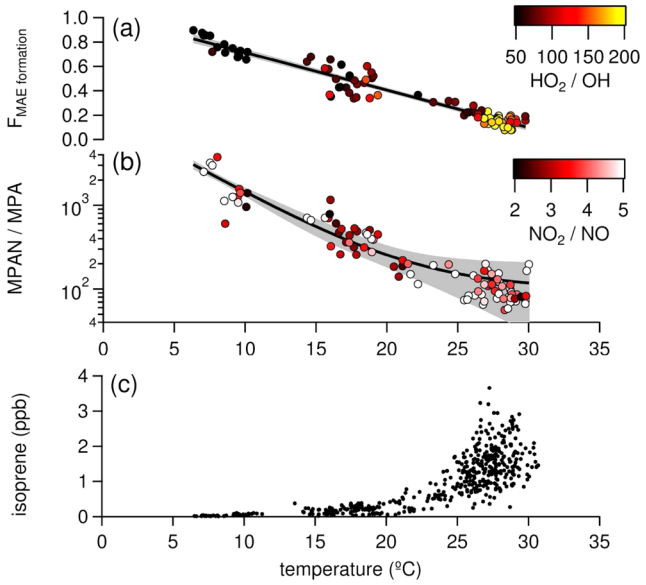

Figure 3. (a) Temperature dependent fractional loss of the MPAN reservoir (MPAN+MPA radical) to reaction with OH relative to loss to NO, HO_2, and RO_2, (FMAE formation) determined for daytime from the APN steady state model. Symbols are colored by the measured HO_2/OH ratio. (b) Temperature dependence of daytime MPAN/MPA radical ratio from the APN steady state model colored by the observed NO_2/NO ratio. (c) Measured isoprene concentrations (ppb) as a function of temperature for both BEARPEX campaigns.

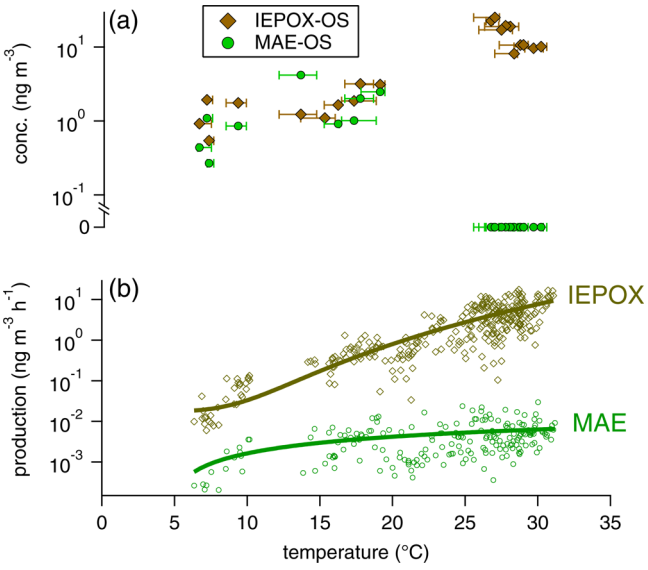

Figure 4. (a) Observed concentrations of the IEPOX- (IEPOX-OS; filled diamonds) and MAE-derived organosulfates (MAE-OS; filled circles) as a function of temperature. Temperatures were the median values during filter collection and the error bars represent the interquartile range of the observed temperature during each filter collection. (b) Calculated production rates (ng m^{-3} h^{-1}) of MAE (open circles) and IEPOX (open diamonds) for both BEARPEX campaigns as a function of temperature. Solid lines are best fit lines.

MPAN (Figures S6 and S7, Supporting Information). To investigate the role the MPAN thermal lifetime has on limiting SOA formation from the OH oxidation of MPAN, we employed a steady state model of acyl peroxy nitrates (APN model) as described in previous work by LaFranchi et al.,[52] constrained by measurements made during both BEARPEX campaigns.

Figure 3a shows the relationship between the observed ambient temperature, measurements of the HO_2/OH ratio, and the ratio of MPAN loss to reaction with OH (the SOA formation pathway) to the MPA loss to reaction with NO, HO_2, and RO_2 ($F_{MAE\ formation}$) determined from the APN model. Figure 3b shows the APN modeled ratio of MPAN to MPA and the measured NO_2/NO ratio as a function of the observed temperature. This figure shows the changing distribution of the MPAN/MPA reservoir as a function of the varying thermal dissociation rate of MPAN. The MPAN/MPA ratio is important for determining the availability of MPAN for reaction with OH and is lower at warmer temperatures and appears almost independent of the NO_2/NO, which would be consistent with the dominance of the thermal decomposition reaction over reformation at higher temperatures.

Low ratios of $F_{MAE\ formation}$ represent conditions when loss of MPAN reservoir species were dominated by reaction of the MPA radical with NO, HO_2, and RO_2 with values of zero indicating all loss forms gas phase products that do not lead to known SOA products from the NO/NO_2 channel. Higher $F_{MAE\ formation}$ ratios are driven by the significance of the MPAN + OH reaction and represent conditions that were more favorable for SOA formation from MAE, with values of unity indicating all MPAN loss is from reaction with OH to form MAE and subsequently SOA. Higher ratios of $F_{MAE\ formation}$ coincide with higher MPAN/MPA ratios (Figure 3b) and lower HO_2/OH ratios (Figure 3a), which both favor the MPAN+OH channel.

Figure 3c shows the temperature dependence of observed isoprene concentrations for both BEARPEX campaigns, which shows that the smallest $F_{MAE\ formation}$ coincides with the highest concentrations of isoprene. The combination of these factors leads to an almost constant production rate of MAE with temperature, which is in contrast to the strong temperature dependence of the IEPOX production rate (Figure 4). Altogether, similar concentrations of the MAE-derived organosulfates might have been expected during both campaigns. However, the negligible concentrations in 2009 indicate there are additional factors that limit the formation of the MAE-derived organosulfate and possibly also SOA from the NO/NO_2 channel.

Role of Aerosol Acidity, Liquid Water Content and Other Processes in Controlling SOA Formation. No correlations were observed between the observed concentrations of the IEPOX- and MAE-derived organosulfates and aerosol pH or liquid water content (LWC), calculated from the E-AIM model (Figure S8, Supporting Information). On average, the pH of the aerosol was 3−5 during both BEARPEX campaigns while the LWC was a factor of 3 higher in 2007 and reached values close to 10 μg m^{-3} on several occasions. In 2009, the LWC was consistently <1 μg m^{-3}. The observation of these organosulfate compounds in aerosol with a pH of ∼4−5 confirms earlier theoretical work that ring-opening epoxide chemistry is kinetically favorable at atmospherically relevant aerosol acidities.[61] The lack of a correlation between aerosol pH and LWC and the observed organosulfate concentrations is in contrast to laboratory experiments, which observed strong dependences of these compounds on aerosol pH and LWC[29] but is consistent with recent ambient observations in the southeast US.[62] However, it is likely that the limited range in these parameters during both campaigns was not sufficient to observe these dependences or that they were formed away from the site and as such would be less correlated with locally measured parameters.

dx.doi.org/10.1021/es4011064 | Environ. Sci. Technol. 2013, 47, 11403−11413

Coincident measurements of gas phase IEPOX and the IEPOX-derived organosulfates in 2009 show that IEPOX was present in substantial excess (~700 times for IEPOX on a molar basis). Laboratory data has shown the branching ratio between the IEPOX-derived organosulfates and the 2-methyl tetrols (the hydrolysis products of IEPOX ring-opening) to range between 5% and 40% for 0.1 to 3 M sulfate solutions.[29] The calculated sulfate molarity of the aerosol, determined from the aerosol sulfate and aerosol volume data, was 1.3 M in 2009 (2.7 M in 2007) (Table 1) representing a sulfate ester yield of 30% in 2009 (40% in 2007). Even after scaling the IEPOX-derived organosulfate concentrations to take account of these additional ring-opening products, gas phase IEPOX was still present in substantial excess (~200 times on a molar basis). This would be consistent with modeling work that showed gas phase oxidation and dry deposition of IEPOX were more important sinks than aerosol formation with less than 1% of the IEPOX ending up as particle phase ring-opening products.[29]

MPAN measurements were made coincidentally with the MAE-derived organosulfates in 2007. Assuming a yield of 20% for MAE from MPAN oxidation[17] and a sulfate ester yield of 40% for the MAE-derived organosulfates suggests that MAE was present with lower excess relative to its organosulfate derivatives (~10 times on a molar basis) than IEPOX. This lower excess of estimated gas phase MAE compared to IEPOX suggests that reactive uptake of MAE may be more efficient or more competitive with gas phase oxidation and/or dry deposition than IEPOX.

To evaluate the relative contributions of the different loss mechanisms (OH oxidation, dry deposition and ring-opening product formation) for IEPOX and MAE in this environment we use the kinetic model described by Eddingsaas et al.,[29] constrained by the measured temperature and OH concentrations and the calculated ranges in the aerosol pH and LWC for BEARPEX. We use the kinetics simulation software Kintecus[63] to follow the decay of IEPOX and MAE for 100 h to ensure complete loss of MAE (IEPOX was completely removed in 30 h).

In the model, loss of IEPOX and MAE are represented by four reactions (shown here for MAE):

$$\mathrm{MAE_g + OH \rightarrow MAE_{ox}} \qquad k_{ox} \tag{2}$$

$$\mathrm{MAE_g \rightarrow MAE_{dd}} \qquad k_{dd} \tag{3}$$

$$\mathrm{MAE_g \leftrightarrow MAE_a} \qquad k_{eq} = k_{par}/k_{vol} \tag{4}$$

$$\mathrm{MAE_a + H^+ \rightarrow MAE_{rop}} \qquad k_{H+} \tag{5}$$

where $\mathrm{MAE_g}$ is gas phase MAE, $\mathrm{MAE_{ox}}$ are gas phase oxidation products of MAE, $\mathrm{MAE_{dd}}$ is dry deposition of MAE, $\mathrm{MAE_a}$ is aerosol phase MAE, $\mathrm{MAE_{rop}}$ is condensed phase ring-opening products of MAE, k_{ox} is the gas phase oxidation rate constant, k_{dd} is the dry deposition rate constant, k_{par} is the rate constant for aerosol partitioning, k_{vol} is the rate constant for vaporization back to the gas phase, and k_{H+} is the acid catalyzed epoxide ring-opening rate constant.

The OH reaction rate of MAE has not been measured, so we estimate it using the EPA's AOPWIN program.[64] The AOPWIN program overpredicted the IEPOX+OH rate constant by 35% so we scaled the MAE+OH rate from AOPWIN by this amount to give an estimate of 1.0×10^{-12} $\mathrm{cm^3\ molecules^{-1}\ s^{-1}}$ (at 298 K), an order of magnitude slower than the IEPOX + OH reaction.[16] The same value was used by Lin et al.[17] to model MAE oxidation in smog chamber experiments giving confidence in its assignment. Using the average measured OH concentrations from BEARPEX, the lifetimes of IEPOX and MAE to OH loss were estimated to be 7 and 90 h, respectively. The deposition rate (k_{dd}) was determined by deposition velocity divided by boundary layer height. Consistent with the work of Eddingsaas et al.,[29] we assume the same deposition velocity for IEPOX and MAE as hydrogen peroxide (1−5 cm $\mathrm{s^{-1}}$; providing an upper limit for this process)[65,66] and reported estimations of the median boundary layer height (600−700 m) during BEARPEX[67] giving a deposition rate of $\sim 4 \times 10^{-5}$ $\mathrm{s^{-1}}$.

Due to the high volatilities of IEPOX (subcooled vapor pressure 4.9×10^{-6} atm; $C^0 = 4.0 \times 10^4$) and MAE (9.2×10^{-5} atm; $C^0 = 7.5 \times 10^5$), gas to particle partitioning into the organic fraction of the aerosol are negligible for both species under typical organic mass loadings (1−10 $\mu\mathrm{g\ m^{-3}}$) in the atmosphere. Vapor pressures were estimated using the group contribution method.[68] However, partitioning of water-soluble organics into the aerosol aqueous phase can occur and are governed by the Henry's law constant (k_H^{cp}). A k_H^{cp} of 1.3×10^8 M $\mathrm{atm^{-1}}$ has been estimated for IEPOX.[28] The Henry's law constant for MAE has not been measured so we estimate it here using EPA's HENRYWIN program.[64] The estimate can be refined by comparison with analogous compounds whose k_H^{cp} values have been measured, e.g., 2-methyl propanoic acid (8.9×10^7 M $\mathrm{atm^{-1}}$)[69] giving an estimate of 7.5×10^6 M $\mathrm{atm^{-1}}$, a factor of 20 lower than IEPOX.

Eddingsaas et al.[29] estimated a ring-opening rate constant (k_{H+}) of 5×10^{-2} $\mathrm{M^{-1}\ s^{-1}}$ for IEPOX and showed that the presence of electron withdrawing groups on the α- and β-carbon(s) to the epoxide slowed down the ring-opening reaction rate by removing electron density from the epoxide oxygen. MAE is different from IEPOX in that it has one less electron withdrawing group. Assuming that carboxylic acid groups behave the same as hydroxyl groups, the ring-opening rate constant for MAE would be ~5 $\mathrm{M^{-1}\ s^{-1}}$, about 2 orders of magnitude faster than IEPOX.[29]

Figure 5 shows a comparison of these loss processes for MAE and IEPOX for BEARPEX 2007 and 2009. As a result of the lower OH rate constant, loss of MAE is dominated by dry deposition, whereas for IEPOX dry deposition and reaction with OH are approximately equivalent. As a result the fraction of MAE that forms ring-opening products is more dependent on the deposition velocity than IEPOX (Figure S9, Supporting Information). In addition, MAE forms one to two orders of magnitude more ring-opening products than IEPOX, depending on the deposition velocity of MAE, and the fraction of ring-opening products (F_{rop}) is larger in 2007 as a result of the higher aerosol LWC (Figure S9, Supporting Information). The lower F_{rop} for IEPOX in 2009 is compensated by the large increase in gas phase IEPOX (~2 orders of magnitude), while the estimated MAE concentrations are similar leading to less MAE ring-opening products in 2009 (Figure 5). This is consistent with our observations, although the magnitude of the change in F_{rop} for MAE between 2007 and 2009 is much less than our observations. This may be the result of lower organosulfate formation as a fraction of ring opening products in 2009 due to lower sulfate molaities and would suggest a stronger dependence of the branching ratio for the MAE-derived organosulfates on sulfate relative to IEPOX. The modeling work presented here is by no means complete and is only meant to provide a means of illustrating the differences between IEPOX and MAE. Further work is needed to observe and quantify MAE in the atmosphere and to better define key parameters (e.g., Henry's Law constant,

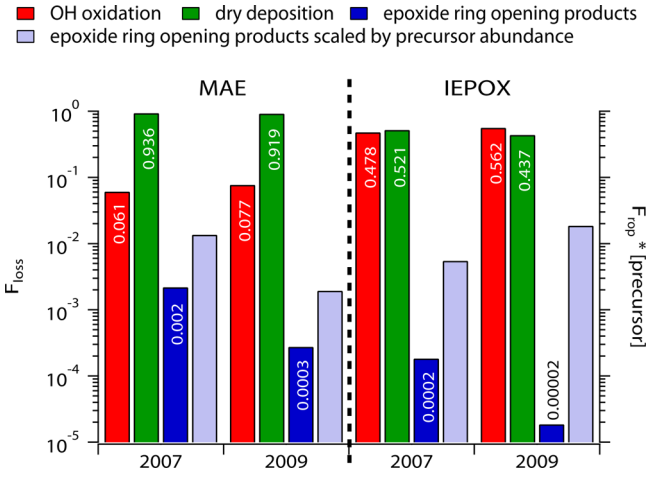

Figure 5. Relative contributions of OH oxidation, dry deposition, and condensed phase ring-opening as sinks (F_{loss}) for MAE and IEPOX as determined from the kinetic model for both BEARPEX campaigns (pH = 4, LWC = 1 μg m^{-3}, OH = 2.8 × 10^6 molecules cm^{-3}, T = 11 °C and boundary layer height = 600 m for 2007 and pH = 4, LWC = 0.1 μg m^{-3}, OH = 3.0 × 10^6 molecules cm^{-3}, T = 28 °C and boundary layer height = 700 m for 2009). Additionally, the fraction forming condensed phase ring-opening products (F_{rop}) were scaled by precursor abundances, 6 (7) and 30 (1000) ppt during 2007 (2009) for MAE and IEPOX, respectively. The abundance of MAE was estimated assuming a 20% yield from MPAN and for 2007 IEPOX was estimated by scaling the isoprene concentrations based on the ratio of IEPOX/isoprene in 2009.

OH rate constant, deposition velocity, and the ring-opening kinetics) that define the fate of MAE (and IEPOX) in the atmosphere.

Atmospheric Implications. Previous work has estimated that isoprene SOA is the largest fraction of total OA in the summertime when isoprene emissions and photochemistry are close to their annual maxima.[70] The strong anti-correlation between the temperature dependence of isoprene concentrations and the fraction of the MPAN reservoir that forms MAE ($F_{MAE\ formation}$) leads to an MAE production rate that is independent of isoprene concentrations. Even the larger fraction of MAE forming condensed phase ring-opening products (F_{rop}) cannot compensate for the lower MAE production rate, relative to IEPOX, at high isoprene concentrations. This indicates that isoprene SOA formation from the HO_2 channel via IEPOX is more important than formation from the NO/NO_2 channel via MAE at the surface. This is supported by observations of higher concentrations of IEPOX-derived SOA tracers relative to MAE-derived SOA tracers at ground sites in summer.[62,70]

However, the strong temperature dependence of the fate of the MPAN reservoir ($F_{MAE\ formation}$) coupled with the known altitudinal dependence of temperature and observations and models showing elevated OH and NO_2 above the boundary layer[71−74] suggests that SOA formation from MAE could be enhanced aloft. Advection of MACR out of the boundary layer and into a cooler temperature regime with available OH and NO_2 would generate MPAN in under conditions that favor MAE formation and SOA from the NO/NO_2 pathway leading to a vertically varying isoprene SOA source. This notation is supported by (i) a recent aircraft study that observed a substantial enhancement in isoprene SOA aloft in the presence of anthropogenic NO_x,[3] and (ii) discrepancies between satellite retrievals of aerosol optical thickness and surface organic aerosol measurements in the southeast US that imply there must be an altitudinal dependence in the SOA source.[4] Additionally, recent observations of 2-MG (the analog of the MAE-derived organosulfate) in the remote North Pacific Ocean and Arctic suggests that the likely longer thermal lifetime of MPAN aloft may also have implications for the long-range transport and subsequent formation of SOA in remote regions of the atmosphere.[75]

■ ASSOCIATED CONTENT

Supporting Information

Experimental methods and additional figures. This material is available free of charge via the Internet at http://pubs.acs.org.

■ AUTHOR INFORMATION

Corresponding Author

*E-mail: dworton@berkeley.edu, Tel. +1-510-643-6449, Fax. +1-510-643-5098.

Notes

The authors declare no competing financial interest.

■ ACKNOWLEDGMENTS

Funding for UCB was provided by the National Science Foundation (NSF, Grants ATM-0922562 and ATM-0639847). DKF, KSD, MJC and JLJ were supported by NSF ATM-0919189. JBG and JDG were partially supported by NSF ATM-0516610. GMW acknowledges support from NASA Earth Systems Science Fellowship NNG-05GP64H and U.S.-EPA STAR Fellowship (FP-91698901). MRB, JMC, JC, and POW were supported by NSF ATM-0934408 and ATM-0934345. Analyses at the University of Aarhus were partially funded by the NSF US-NORDIC BSOA workshop program. The authors acknowledge Sierra Pacific Industries for the use of their land and the Blodgett Forest Research Station for cooperation in facilitating this research. The authors thank S. S. Cliff (University of California, Davis) for the loan of the high volume filter sampler, N. C. Bouvier-Brown (Loyola Marymount University, Los Angeles) for assistance with filter collection, J. Murphy (University of Toronto) for initial discussions about the E-AIM model, N. Eddingsaas (Caltech) for providing the BEPOX-derived organosulfate standard, D. Covert (University of Washington) for providing the SMPS measurements in 2009 and M. Chan and K. Schilling (Caltech) for their assistance with filter extractions and UPLC/ESI-HR-TOFMS analyses.

■ REFERENCES

(1) Hallquist, M.; Wenger, J. C.; Baltensperger, U.; Rudich, Y.; Simpson, D.; Claeys, M.; Dommen, J.; Donahue, N. M.; George, C.; Goldstein, A. H.; Hamilton, J. F.; Herrmann, H.; Hoffmann, T.; Iinuma, Y.; Jang, M.; Jenkin, M. E.; Jimenez, J. L.; Kiendler-Scharr, A.; Maenhaut, W.; McFiggans, G.; Mentel, T. F.; Monod, A.; Prevot, A. S. H.; Seinfeld, J. H.; Surratt, J. D.; Szmigielski, R.; Wildt, J. The formation, properties and impact of secondary organic aerosol: current and emerging issues. *Atmos. Chem. Phys.* **2009**, *9* (14), 5155−5236.

(2) Jimenez, J. L.; Canagaratna, M. R.; Donahue, N. M.; Prevot, A. S. H.; Zhang, Q.; Kroll, J. H.; DeCarlo, P. F.; Allan, J. D.; Coe, H.; Ng, N. L.; Aiken, A. C.; Docherty, K. S.; Ulbrich, I. M.; Grieshop, A. P.; Robinson, A. L.; Duplissy, J.; Smith, J. D.; Wilson, K. R.; Lanz, V. A.; Hueglin, C.; Sun, Y. L.; Tian, J.; Laaksonen, A.; Raatikainen, T.; Rautiainen, J.; Vaattovaara, P.; Ehn, M.; Kulmala, M.; Tomlinson, J. M.; Collins, D. R.; Cubison, M. J.; Dunlea, E. J.; Huffman, J. A.; Onasch, T. B.; Alfarra, M. R.; Williams, P. I.; Bower, K.; Kondo, Y.; Schneider, J.; Drewnick, F.; Borrmann, S.; Weimer, S.; Demerjian, K.; Salcedo, D.; Cottrell, L.; Griffin, R.; Takami, A.; Miyoshi, T.; Hatakeyama, S.; Shimono, A.; Sun, J. Y.; Zhang, Y. M.; Dzepina, K.; Kimmel, J. R.;

Sueper, D.; Jayne, J. T.; Herndon, S. C.; Trimborn, A. M.; Williams, L. R.; Wood, E. C.; Middlebrook, A. M.; Kolb, C. E.; Baltensperger, U.; Worsnop, D. R. Evolution of Organic Aerosols in the Atmosphere. *Science* **2009**, *326* (5959), 1525−1529.

(3) Shilling, J. E.; Zaveri, R. A.; Fast, J. D.; Kleinman, L.; Alexander, M. L.; Canagaratna, M. R.; Fortner, E.; Hubbe, J. M.; Jayne, J. T.; Sedlacek, A.; Setyan, A.; Springston, S.; Worsnop, D. R.; Zhang, Q. Enhanced SOA formation from mixed anthropogenic and biogenic emissions during the CARES campaign. *Atmos. Chem. Phys.* **2013**, *13*, 2091−2113.

(4) Goldstein, A. H.; Koven, C. D.; Heald, C. L.; Fung, I. Y. Biogenic carbon and anthropogenic pollutants combine to form a cooling haze over the southeastern United States. *Proc. Natl. Acad. Sci. U.S.A.* **2009**, *106* (22), 8835−8840.

(5) Carlton, A. G.; Pinder, R. W.; Bhave, P. V.; Pouliot, G. A. To What Extent Can Biogenic SOA be Controlled? *Environ. Sci. Technol.* **2010**, *44* (9), 3376−3380.

(6) Spracklen, D. V.; Jimenez, J. L.; Carslaw, K. S.; Worsnop, D. R.; Evans, M. J.; Mann, G. W.; Zhang, Q.; Canagaratna, M. R.; Allan, J.; Coe, H.; McFiggans, G.; Rap, A.; Forster, P. Aerosol mass spectrometer constraint on the global secondary organic aerosol budget. *Atmos. Chem. Phys.* **2011**, *11* (23), 12109−12136.

(7) Surratt, J. D.; Lewandowski, M.; Offenberg, J. H.; Jaoui, M.; Kleindienst, T. E.; Edney, E. O.; Seinfeld, J. H. Effect of acidity on secondary organic aerosol formation from isoprene. *Environ. Sci. Technol.* **2007**, *41* (15), 5363−5369.

(8) Fry, J. L.; Kiendler-Scharr, A.; Rollins, A. W.; Wooldridge, P. J.; Brown, S. S.; Fuchs, H.; Dube, W.; Mensah, A.; dal Maso, M.; Tillmann, R.; Dorn, H. P.; Brauers, T.; Cohen, R. C. Organic nitrate and secondary organic aerosol yield from NO3 oxidation of beta-pinene evaluated using a gas-phase kinetics/aerosol partitioning model. *Atmos. Chem. Phys.* **2009**, *9* (4), 1431−1449.

(9) Carlton, A. G.; Wiedinmyer, C.; Kroll, J. H. A review of Secondary Organic Aerosol (SOA) formation from isoprene. *Atmos. Chem. Phys.* **2009**, *9* (14), 4987−5005.

(10) Guenther, A.; Karl, T.; Harley, P.; Wiedinmyer, C.; Palmer, P. I.; Geron, C. Estimates of global terrestrial isoprene emissions using MEGAN (Model of Emissions of Gases and Aerosols from Nature). *Atmos. Chem. Phys.* **2006**, *6*, 3181−3210.

(11) Atkinson, R.; Arey, J. Gas-phase tropospheric chemistry of biogenic volatile organic compounds: a review. *Atmos. Environ.* **2003**, *37*, S197−S219.

(12) Kroll, J. H.; Ng, N. L.; Murphy, S. M.; Flagan, R. C.; Seinfeld, J. H. Secondary organic aerosol formation from isoprene photooxidation. *Environ. Sci. Technol.* **2006**, *40* (6), 1869−1877.

(13) Chan, A. W. H.; Chan, M. N.; Surratt, J. D.; Chhabra, P. S.; Loza, C. L.; Crounse, J. D.; Yee, L. D.; Flagan, R. C.; Wennberg, P. O.; Seinfeld, J. H. Role of aldehyde chemistry and NOx concentrations in secondary organic aerosol formation. *Atmos. Chem. Phys.* **2010**, *10* (15), 7169−7188.

(14) Kroll, J. H.; Ng, N. L.; Murphy, S. M.; Flagan, R. C.; Seinfeld, J. H. Secondary organic aerosol formation from isoprene photooxidation under high-NO(x) conditions. *Geophys. Res. Lett.* **2005**, *32* (18), L18808.

(15) Surratt, J. D.; Chan, A. W. H.; Eddingsaas, N. C.; Chan, M.; Loza, C. L.; Kwan, A. J.; Hersey, S. P.; Flagan, R. C.; Wennberg, P. O.; Seinfeld, J. H. Reactive intermediates revealed in secondary organic aerosol formation from isoprene. *Proc. Natl. Acad. Sci. U.S.A.* **2010**, *107* (15), 6640−6645.

(16) Paulot, F.; Crounse, J. D.; Kjaergaard, H. G.; Kuerten, A.; St Clair, J. M.; Seinfeld, J. H.; Wennberg, P. O. Unexpected Epoxide Formation in the Gas-Phase Photooxidation of Isoprene. *Science* **2009**, *325* (5941), 730−733.

(17) Lin, Y.-H.; Zhang, H.; Pye, H. O. T.; Zhang, Z.; Marth, W. J.; Park, S.; Arashiro, M.; Cui, T.; Budisulistiorini, H.; Sexton, K. G.; Vizuete, W.; Xie, Y.; Luecken, D. J.; Piletic, I. R.; Edney, E. O.; Bartolotti, L. J.; Gold, A.; Surratt, J. D. Epoxide as a precursor to secondary organic aerosol formation from isoprene photooxidation in the presence of nitrogen oxides. *Proc. Natl. Acad. Sci. U.S.A.* **2013**, *110* (17), 6718−6723.

(18) Liu, Y. J.; Herdlinger-Blatt, I.; McKinney, K. A.; Martin, S. T. Production of methyl vinyl ketone and methacrolein via the hydroperoxyl pathway of isoprene oxidation. *Atmos. Chem. Phys.* **2013**, *13* (11), 5715−5730.

(19) Lin, Y.-H.; Zhang, Z.; Docherty, K. S.; Zhang, H.; Budisulistiorini, S. H.; Rubitschun, C. L.; Shaw, S. L.; Knipping, E. M.; Edgerton, E. S.; Kleindienst, T. E.; Gold, A.; Surratt, J. D. Isoprene Epoxydiols as Precursors to Secondary Organic Aerosol Formation: Acid-Catalyzed Reactive Uptake Studies with Authentic Compounds. *Environ. Sci. Technol.* **2012**, *46* (1), 250−258.

(20) Surratt, J. D.; Kroll, J. H.; Kleindienst, T. E.; Edney, E. O.; Claeys, M.; Sorooshian, A.; Ng, N. L.; Offenberg, J. H.; Lewandowski, M.; Jaoui, M.; Flagan, R. C.; Seinfeld, J. H. Evidence for organosulfates in secondary organic aerosol. *Environ. Sci. Technol.* **2007**, *41* (2), 517−527.

(21) Claeys, M.; Graham, B.; Vas, G.; Wang, W.; Vermeylen, R.; Pashynska, V.; Cafmeyer, J.; Guyon, P.; Andreae, M. O.; Artaxo, P.; Maenhaut, W. Formation of secondary organic aerosols through photooxidation of isoprene. *Science* **2004**, *303* (5661), 1173−1176.

(22) Szmigielski, R.; Surratt, J. D.; Vermeylen, R.; Szmigielska, K.; Kroll, J. H.; Ng, N. L.; Murphy, S. M.; Sorooshian, A.; Seinfeld, J. H.; Claeys, M. Characterization of 2-methylglyceric acid oligomers in secondary organic aerosol formed from the photooxidation of isoprene using trimethylsilylation and gas chromatography/ion trap mass spectrometry. *J. Mass Spectrom.* **2007**, *42* (1), 101−116.

(23) Surratt, J. D.; Murphy, S. M.; Kroll, J. H.; Ng, a. L. N.; Hildebrandt, L.; Sorooshian, A.; Szmigielski, R.; Vermeylen, R.; Maenhaut, W.; Claeys, M.; Flagan, R. C.; Seinfeld, J. H. Chemical composition of secondary organic aerosol formed from the photooxidation of isoprene. *J. Phys. Chem. A* **2006**, *110* (31), 9665−9690.

(24) Edney, E. O.; Kleindienst, T. E.; Jaoui, M.; Lewandowski, M.; Offenberg, J. H.; Wang, W.; Claeys, M. Formation of 2-methyl tetrols and 2-methylglyceric acid in secondary organic aerosol from laboratory irradiated isoprene/NO(X)/SO(2)/air mixtures and their detection in ambient PM(2.5) samples collected in the eastern United States. *Atmos. Environ.* **2005**, *39* (29), 5281−5289.

(25) Galloway, M. M.; Huisman, A. J.; Yee, L. D.; Chan, A. W. H.; Loza, C. L.; Seinfeld, J. H.; Keutsch, F. N. Yields of oxidized volatile organic compounds during the OH radical initiated oxidation of isoprene, methyl vinyl ketone, and methacrolein under high-NOx conditions. *Atmos. Chem. Phys.* **2011**, *11* (21), 10779−10790.

(26) Carlton, A. G.; Turpin, B. J.; Altieri, K. E.; Seitzinger, S.; Reff, A.; Lim, H.-J.; Ervens, B. Atmospheric oxalic acid and SOA production from glyoxal: Results of aqueous photooxidation experiments. *Atmos. Environ.* **2007**, *41* (35), 7588−7602.

(27) McNeill, V. F.; Woo, J. L.; Kim, D. D.; Schwier, A. N.; Wannell, N. J.; Sumner, A. J.; Barakat, J. M. Aqueous-Phase Secondary Organic Aerosol and Organosulfate Formation in Atmospheric Aerosols: A Modeling Study. *Environ. Sci. Technol.* **2012**, *46* (15), 8075−8081.

(28) Minerath, E. C.; Casale, M. T.; Elrod, M. J. Kinetics feasibility study of alcohol sulfate esterification reactions in tropospheric aerosols. *Environ. Sci. Technol.* **2008**, *42* (12), 4410−4415.

(29) Eddingsaas, N. C.; VanderVelde, D. G.; Wennberg, P. O. Kinetics and Products of the Acid-Catalyzed Ring-Opening of Atmospherically Relevant Butyl Epoxy Alcohols. *J. Phys. Chem. A* **2010**, *114* (31), 8106−8113.

(30) Hu, K. S.; Darer, A. I.; Elrod, M. J. Thermodynamics and kinetics of the hydrolysis of atmospherically relevant organonitrates and organosulfates. *Atmos. Chem. Phys.* **2011**, *11* (16), 8307−8320.

(31) Tanner, R. L.; Olszyna, K. J.; Edgerton, E. S.; Knipping, E.; Shaw, S. L. Searching for evidence of acid-catalyzed enhancement of secondary organic aerosol formation using ambient aerosol data. *Atmos. Environ.* **2009**, *43* (21), 3440−3444.

(32) Worton, D. R.; Goldstein, A. H.; Farmer, D. K.; Docherty, K. S.; Jimenez, J. L.; Gilman, J. B.; Kuster, W. C.; de Gouw, J.; Williams, B. J.; Kreisberg, N. M.; Hering, S. V.; Bench, G.; McKay, M.; Kristensen, K.; Glasius, M.; Surratt, J. D.; Seinfeld, J. H. Origins and composition of fine atmospheric carbonaceous aerosol in the Sierra Nevada Mountains, California. *Atmos. Chem. Phys.* **2011**, *11* (19), 10219−10241.

(33) Goldstein, A. H.; Hultman, N. E.; Fracheboud, J. M.; Bauer, M. R.; Panek, J. A.; Xu, M.; Qi, Y.; Guenther, A. B.; Baugh, W. Effects of climate variability on the carbon dioxide, water, and sensible heat fluxes above a ponderosa pine plantation in the Sierra Nevada (CA). *Agricultural and Forest Meteorology* **2000**, *101* (2−3), 113−129.
(34) Murphy, J. G.; Day, A.; Cleary, P. A.; Wooldridge, P. J.; Cohen, R. C. Observations of the diurnal and seasonal trends in nitrogen oxides in the western Sierra Nevada. *Atmos. Chem. Phys.* **2006**, *6*, 5321−5338.
(35) Dreyfus, G. B.; Schade, G. W.; Goldstein, A. H. Observational constraints on the contribution of isoprene oxidation to ozone production on the western slope of the Sierra Nevada, California. *J. Geophys. Res. [Atmos.]* **2002**, *107* (D19), 4365.
(36) Surratt, J. D.; Gomez-Gonzalez, Y.; Chan, A. W. H.; Vermeylen, R.; Shahgholi, M.; Kleindienst, T. E.; Edney, E. O.; Offenberg, J. H.; Lewandowski, M.; Jaoui, M.; Maenhaut, W.; Claeys, M.; Flagan, R. C.; Seinfeld, J. H. Organosulfate formation in biogenic secondary organic aerosol. *J. Phys. Chem. A* **2008**, *112* (36), 8345−8378.
(37) Cech, N. B.; Krone, J. R.; Enke, C. G. Predicting electrospray response from chromatographic retention time. *Anal. Chem.* **2001**, *73* (2), 208−213.
(38) Gilman, J. B.; Burkhart, J. F.; Lerner, B. M.; Williams, E. J.; Kuster, W. C.; Goldan, P. D.; Murphy, P. C.; Warneke, C.; Fowler, C.; Montzka, S. A.; Miller, B. R.; Miller, L.; Oltmans, S. J.; Ryerson, T. B.; Cooper, O. R.; Stohl, A.; de Gouw, J. A. Ozone variability and halogen oxidation within the Arctic and sub-Arctic springtime boundary layer. *Atmos. Chem. Phys.* **2010**, *10* (21), 10223−10236.
(39) Park, C.; Schade, G. W.; Boedeker, I. Characteristics of the flux of isoprene and its oxidation products in an urban area. *J. Geophys. Res. [Atmos.]* **2011**, *116*, D21303.
(40) Park, C.; Schade, G. W.; Boedeker, I. Flux measurements of volatile organic compounds by the relaxed eddy accumulation method combined with a GC-FID system in urban Houston, Texas. *Atmos. Environ.* **2010**, *44* (21−22), 2605−2614.
(41) Wolfe, G. M.; Thornton, J. A.; Yatavelli, R. L. N.; McKay, M.; Goldstein, A. H.; LaFranchi, B.; Min, K. E.; Cohen, R. C. Eddy covariance fluxes of acyl peroxy nitrates (PAN, PPN and MPAN) above a Ponderosa pine forest. *Atmos. Chem. Phys.* **2009**, *9* (2), 615−634.
(42) Day, D. A.; Wooldridge, P. J.; Dillon, M. B.; Thornton, J. A.; Cohen, R. C. A thermal dissociation laser-induced fluorescence instrument for in situ detection of NO 2, peroxy nitrates, alkyl nitrates, and HNO 3. *J. Geophys. Res.* **2002**, *107* (D5-D6), ACH4−1−4−14.
(43) Crounse, J. D.; McKinney, K. A.; Kwan, A. J.; Wennberg, P. O. Measurement of gas-phase hydroperoxides by chemical ionization mass spectrometry. *Anal. Chem.* **2006**, *78* (19), 6726−6732.
(44) Day, D. A.; Farmer, D. K.; Goldstein, A. H.; Wooldridge, P. J.; Minejima, C.; Cohen, R. C. Observations of NOx, $Aigma$PNs, $Aigma$ANs, and HNO3 at a Rural Site in the California Sierra Nevada Mountains: summertime diurnal cycles. *Atmos. Chem. Phys.* **2009**, *9* (14), 4879−4896.
(45) Thornton, J. A.; Wooldridge, P. J.; Cohen, R. C. Atmospheric NO2: In situ laser-induced fluorescence detection at parts per trillion mixing ratios. *Anal. Chem.* **2000**, *72* (3), 528−539.
(46) Ridley, B. A.; Grahek, F. E. A small, low flow, high-sensitivity reaction vessel for NO chemiluminescence detectors. *Journal of Atmospheric and Oceanic Technology* **1990**, *7* (2), 307−311.
(47) Drummond, J. W.; Volz, A.; Ehhalt, D. H. An optimized chemiluminescence detector for tropospheric NO measurements. *J. Atmos. Chem.* **1985**, *2* (3), 287−306.
(48) Faloona, I. C.; Tan, D.; Lesher, R. L.; Hazen, N. L.; Frame, C. L.; Simpas, J. B.; Harder, H.; Martinez, M.; Di Carlo, P.; Ren, X. R.; Brune, W. H. A laser-induced fluorescence instrument for detecting tropospheric OH and HO2: Characteristics and calibration. *J. Atmos. Chem.* **2004**, *47* (2), 139−167.
(49) Kovacs, T. A.; Brune, W. H. Total OH loss rate measurement. *J. Atmos. Chem.* **2001**, *39* (2), 105−122.
(50) Farmer, D. K.; Kimmel, J. R.; Phillips, G.; Docherty, K. S.; Worsnop, D. R.; Sueper, D.; Nemitz, E.; Jimenez, J. L. Eddy covariance measurements with high-resolution time-of-flight aerosol mass spectrometry: a new approach to chemically resolved aerosol fluxes. *Atmospheric Measurement Techniques* **2011**, *4* (6), 1275−1289.
(51) Russell, L. M. Aerosol organic-mass-to-organic-carbon ratio measurements. *Environ. Sci. Technol.* **2003**, *37* (13), 2982−2987.
(52) LaFranchi, B. W.; Wolfe, G. M.; Thornton, J. A.; Harrold, S. A.; Browne, E. C.; Min, K. E.; Wooldridge, P. J.; Gilman, J. B.; Kuster, W. C.; Goldan, P. D.; de Gouw, J. A.; McKay, M.; Goldstein, A. H.; Ren, X.; Mao, J.; Cohen, R. C. Closing the peroxy acetyl nitrate budget: observations of acyl peroxy nitrates (PAN, PPN, and MPAN) during BEARPEX 2007. *Atmos. Chem. Phys.* **2009**, *9* (19), 7623−7641.
(53) Clegg, S. L.; Brimblecombe, P.; Wexler, A. S. Thermodynamic model of the system H+-NH4+-SO42–NO3–H2O at tropospheric temperatures. *J. Phys. Chem. A* **1998**, *102* (12), 2137−2154.
(54) Wexler, A. S.; Clegg, S. L. Atmospheric aerosol models for systems including the ions H+, NH4+, Na+, SO42-, NO3-,Cl-, Br-, and H2O. *J. Geophys. Res. [Atmos.]* **2002**, *107* (D14), 4207.
(55) Yao, X. H.; Ling, T. Y.; Fang, M.; Chan, C. K. Comparison of thermodynamic predictions for in situ pH in PM2.5. *Atmos. Environ.* **2006**, *40* (16), 2835−2844.
(56) Speer, R. E.; Edney, E. O.; Kleindienst, T. E. Impact of organic compounds on the concentrations of liquid water in ambient PM2.5. *J. Aerosol Sci.* **2003**, *34* (1), 63−77 Pii s0021−8502(02)00152−0.
(57) Aggarwal, S. G.; Mochida, M.; Kitamori, Y.; Kawamura, K. Chemical closure study on hygroscopic properties of urban aerosol particles in Sapporo, Japan. *Environ. Sci. Technol.* **2007**, *41* (20), 6920−6925.
(58) Liu, J. M.; Zhang, X. L.; Parker, E. T.; Veres, P. R.; Roberts, J. M.; de Gouw, J. A.; Hayes, P. L.; Jimenez, J. L.; Murphy, J. G.; Ellis, R. A.; Huey, L. G.; Weber, R. J. On the gas-particle partitioning of soluble organic aerosol in two urban atmospheres with contrasting emissions: 2. Gas and particle phase formic acid. *J. Geophys. Res. [Atmos.]* **2012**, *117*, D00v21.
(59) Guenther, A. B.; Zimmerman, P. R.; Harley, P. C.; Monson, R. K.; Fall, R. Isoprene and monoterpene emission rate variability - model evaluations and sensivity analyses. *J. Geophys. Res. [Atmos.]* **1993**, *98* (D7), 12609−12617.
(60) Roberts, J. M.; Bertman, S. B. The thermal decomposition of peroxyacetic nitric anhydride (PAN)and peroxymethacylic nitric anhydride (MPAN). *Int. J. Chem. Kinet.* **1992**, *24* (3), 297−307.
(61) Darer, A. I.; Cole-Filipiak, N. C.; O'Connor, A. E.; Elrod, M. J. Formation and Stability of Atmospherically Relevant Isoprene-Derived Organosulfates and Organonitrates. *Environ. Sci. Technol.* **2011**, *45* (5), 1895−1902.
(62) Lin, Y. H.; Knipping, E. M.; Edgerton, E. S.; Shaw, S. L.; Surratt, J. D. Investigating the influences of SO2 and NH3 levels on isoprene-derived secondary organic aerosol formation using conditional sampling approaches. *Atmos. Chem. Phys. Discuss.* **2013**, *13* (2), 3095−3134.
(63) Ianni, J. C. Windows Version 2.80, www.kintecus.com.
(64) *USEPA Estimation Programs Interface Suite for Microsoft® Windows*, v 4.11; United States Environmental Protection Agency, Washington, DC, USA.
(65) Stickler, A.; Fischer, H.; Bozem, H.; Gurk, C.; Schiller, C.; Martinez-Harder, M.; Kubistin, D.; Harder, H.; Williams, J.; Eerdekens, G.; Yassaa, N.; Ganzeveld, L.; Sander, R.; Lelieveld, J. Chemistry, transport and dry deposition of trace gases in the boundary layer over the tropical Atlantic Ocean and the Guyanas during the GABRIEL field campaign. *Atmos. Chem. Phys.* **2007**, *7* (14), 3933−3956.
(66) Valverde-Canossa, J.; Ganzeveld, L.; Rappenglueck, B.; Steinbrecher, R.; Klemm, O.; Schuster, G.; Moortgat, G. K. First measurements of H_2O_2 and organic peroxides surface fluxes by the relaxed eddy-accumulation technique. *Atmos. Environ.* **2006**, *40*, S55−S67.
(67) Choi, W.; Faloona, I. C.; McKay, M.; Goldstein, A. H.; Baker, B. Estimating the atmospheric boundary layer height over sloped, forested terrain from surface spectral analysis during BEARPEX. *Atmos. Chem. Phys.* **2011**, *11* (14), 6837−6853.
(68) Pankow, J. F.; Asher, W. E. SIMPOL.1: a simple group contribution method for predicting vapor pressures and enthalpies of

vaporization of multifunctional organic compounds. *Atmos. Chem. Phys.* **2008**, *8* (10), 2773−2796.
(69) Khan, I.; Brimblecombe, P.; Clegg, S. L. Solubilities of pyruvic acid and the lower (C1-C6) carboxylic acids - experimental determination of equilbrium vapor pressures above pure aqueous and salt solutions. *J. Atmos. Chem.* **1995**, *22* (3), 285−302.
(70) Kleindienst, T. E.; Jaoui, M.; Lewandowski, M.; Offenberg, J. H.; Lewis, C. W.; Bhave, P. V.; Edney, E. O. Estimates of the contributions of biogenic and anthropogenic hydrocarbons to secondary organic aerosol at a southeastern US location. *Atmos. Environ.* **2007**, *41* (37), 8288−8300.
(71) Brown, S. S.; Dube, W. P.; Osthoff, H. D.; Stutz, J.; Ryerson, T. B.; Wollny, A. G.; Brock, C. A.; Warneke, C.; de Gouw, J. A.; Atlas, E.; Neuman, J. A.; Holloway, J. S.; Lerner, B. M.; Williams, E. J.; Kuster, W. C.; Goldan, P. D.; Angevine, W. M.; Trainer, M.; Fehsenfeld, F. C.; Ravishankara, A. R. Vertical profiles in NO 3 and N 2O 5 measured from an aircraft: results from the NOAA P-3 and surface platforms during the New England Air Quality Study 2004. *J. Geophys. Res. [Atmos.]* **2007**, *112* (D22), 1−17.
(72) Ren, X.; Olson, J. R.; Crawford, J. H.; Brune, W. H.; Mao, J.; Long, R. B.; Chen, Z.; Chen, G.; Avery, M. A.; Sachse, G. W.; Barrick, J. D.; Diskin, G. S.; Huey, L. G.; Fried, A.; Cohen, R. C.; Heikes, B.; Wennberg, P. O.; Singh, H. B.; Blake, D. R.; Shetter, R. E. HOx chemistry during INTEX-A 2004: Observation, model calculation, and comparison with previous studies. *J. Geophys. Res. [Atmos.]* **2008**, *113* (D5), D05310.
(73) Spivakovsky, C. M.; Logan, J. A.; Montzka, S. A.; Balkanski, Y. J.; Foreman-Fowler, M.; Jones, D. B. A.; Horowitz, L. W.; Fusco, A. C.; Brenninkmeijer, C. A. M.; Prather, M. J.; Wofsy, S. C.; McElroy, M. B. Three-dimensional climatological distribution of tropospheric OH: Update and evaluation. *J. Geophys. Res. [Atmos.]* **2000**, *105* (D7), 8931−8980.
(74) Horowitz, L. W.; Walters, S.; Mauzerall, D. L.; Emmons, L. K.; Rasch, P. J.; Granier, C.; Tie, X. X.; Lamarque, J. F.; Schultz, M. G.; Tyndall, G. S.; Orlando, J. J.; Brasseur, G. P. A global simulation of tropospheric ozone and related tracers: Description and evaluation of MOZART, version 2. *J. Geophys. Res. [Atmos.]* **2003**, *108* (D24), 4784.
(75) Ding, X.; Wang, X.; Xie, Z.; Zhang, Z.; Sun, L. Impacts of Siberian Biomass Burning on Organic Aerosols over the North Pacific Ocean and the Arctic: Primary and Secondary Organic Tracers. *Environ. Sci. Technol.* **2013**, *47*, 3149.